Original Article

MR neurography of lumbosacral nerve roots for differentiating chronic inflammatory demyelinating polyneuropathy from acquired axonal polyneuropathies: a cross-sectional study

Fei Wu[1#], Weiwei Wang[1#], Yang Yang[1#], Chong Li[2], Jie Wu[1], Hanqiu Liu[1*], Yan Ren[1*]

[1]Department of Radiology, Huashan Hospital, Fudan University, Shanghai, China; [2]Department of Radiology, Shijiazhuang People's Hospital, Shijiazhuang, China

Contributions: (I) Conception and design: F Wu, Y Ren, H Liu; (II) Administrative support: H Liu; (III) Provision of study patients: F Wu, W Wang, C Li, Y Yang; (IV) Collection and assembly of data: F Wu, W Wang, J Wu; (V) Data analysis and interpretation: W Wang, Y Ren; (VI) Manuscript writing: All authors; (VII) Final approval of manuscript: All authors.

[#]These authors contributed equally to this work and should be considered as co-first authors.

[*]These authors contributed equally to this work.

Correspondence to: Yan Ren. Department of Radiology, Huashan Hospital, Fudan University, 12 Middle Wulumuqi Rd, Shanghai, 20040, China. Email: renyan_richard@aliyun.com; Hanqiu Liu. Department of Radiology, Huashan Hospital, Fudan University, 12 Middle Wulumuqi Rd, Shanghai, 20040, China. Email: drhancher@163.com.

Background: Magnetic resonance (MR) neurography is an imaging technique focused on the peripheral nerves. Its role in the diagnosis and differential diagnosis of chronic inflammatory demyelinating polyneuropathy (CIDP) has yet to be investigated. This study explored the value of MR neurography in identifying CIDP and differentiating it from acquired axonal polyneuropathies.

Methods: In this study, 20 patients with CIDP, 10 patients with acquired axonal polyneuropathies, and 20 healthy controls were prospectively enrolled. Three-dimensional T2-weighted image fat-suppressed and diffusion tensor imaging sequences of the lumbosacral plexus were completed in all participants. The cross-sectional area (CSA) and diffusion parameters, including the fractional anisotropy (FA) and apparent diffusion coefficient (ADC) of the L3 to S1 nerve roots, were measured and compared across the 3 groups using Kruskal-Wallis 1-way analysis of variance. Receiver operating characteristic (ROC) curves were plotted to determine the value of CSA and diffusion parameters in the diagnosis and differential diagnosis of CIDP.

Results: CSA and ADC increased in CIDP patients but didn't differ between patients with axonal polyneuropathies and healthy controls [CAS: 45.35±23.889, 22.25±3.878, 22.81±4.079 mm^2, ADC: (1.64±0.269)×10^{-3}, (1.37±0.204)×10^{-3} and (1.39±0.156)×10^{-3} mm^2/s, in CIDP, axonal polyneuropathies and healthy controls, respectively, both P<0.001]. Compared with healthy controls, FA reduced in patients with CIDP and axonal polyneuropathies but no difference was observed in the two groups (FA: 0.24±0.053, 0.27±0.014 and 0.32±0.045, in CIDP, axonal polyneuropathies and healthy controls, respectively, P<0.001). To identify CIDP, ROC analysis showed that FA had better efficiency with cut-off value of 0.278 and sensitivity and specificity of 85% and 90% respectively. To differentiate CIDP from axonal polyneuropathies, CSA had better diagnostic accuracy with cut-off value of 29.46 mm^2 and sensitivity and specificity of 75% and 100% respectively.

Conclusions: CSA and ADC values of lumbosacral nerve roots can help to identify patients with CIDP and further distinguish them from patients with axonal polyneuropathies. FA decreased in both types of polyneuropathies and may thus have limited value in the discrimination of the 2 types of neuropathies.

Keywords: Chronic inflammatory demyelinating polyneuropathy (CIDP); axonal degeneration; lumbosacral plexus; magnetic resonance imaging; diffusion tensor imaging

Submitted Feb 17, 2022. Accepted for publication Jul 08, 2022.
doi: 10.21037/qims-22-156
View this article at: https://dx.doi.org/10.21037/qims-22-156

Introduction

Chronic inflammatory demyelinating polyneuropathy (CIDP) is an immune-mediated peripheral nerve disorder that typically manifests as symmetric weakness and sensory dysfunction of the extremities (1). Early identification and precise diagnosis are important because CIDP is clinically treatable, and timely therapy can prevent irreversible secondary axonal degeneration (2). In the diagnostic workup, a crucial step is to differentiate CIDP from axonal polyneuropathies (PNPs) on the basis of a nerve conduction study since it is the most common chronic acquired demyelinating PNP and shares similar clinical manifestations with axonal PNPs (2,3). Generally, the electrophysiological signs of demyelinating PNPs include the slowing of motor nerve conduction velocity and the lengthening of distal motor and F-wave minimal latencies. Meanwhile, characteristic signs of axonal PNPs include reduced amplitudes of compound muscle action and sensory nerve action potentials. However, reduced amplitudes can also be found in demyelinating PNPs, as the chronic proximal demyelinating lesions frequently induce distal axon degeneration and the conduction velocity in axonal PNPs can also be reduced, facts which produce controversy concerning the electrophysiological distinctions between axonal and demyelinating PNPs (2,4,5). Moreover, nerve conduction study may lead to physical discomfort in patients, and its sensitivity and specificity are limited by a number of factors, such as temperature, age, height, and operator experience (2).

Nerve imaging techniques, including high resolution ultrasonography (HRUS) and magnetic resonance neurography (MRN), have proven valuable in the diagnosis of PNPs (6). HRUS allows evaluation of superficial peripheral nerves from the perspective of nerve size and echogenicity in a short window of time. Previous studies have found distinctive sonographic patterns of peripheral nerves in acquired demyelinating and axonal PNPs and thus can further be used to differentiate CIDP from axonal PNPs (5,7-9). MRN is a nerve imaging technique of the peripheral nerves and encompasses a T2-weighted image (T2WI) fat-suppressed sequence and a diffusion tensor imaging (DTI) sequence (10). The former allows a direct depiction of peripheral nerve structure, especially in deep anatomical regions, and the latter is a quantitative approach used to detect microstructural alterations by yielding diffusion parameters (11). To date, a number of studies have investigated the diagnostic potential of MRN in CIDP (12-15). However, most of these studies enrolled only healthy volunteers as the control group and few included clinically relevant controls, in particular axonal PNPs (1,16). Therefore, in this study, we used a 3-dimensional (3D) T2WI fat-suppressed sequence and a DTI sequence to visualize the lumbosacral nerve roots in patients with CIDP and axonal PNPs as well as in healthy volunteers to ascertain the value of MRN in the diagnosis and differential diagnosis of CIDP. We present the following article in accordance with the STROBE reporting checklist (available at https://qims.amegroups.com/article/view/10.21037/qims-22-156/rc).

Methods

Participants

This study was conducted in accordance with the Declaration of Helsinki (as revised in 2013). The study was approved by the institutional ethics board of Huashan Hospital, and informed consent was given by all participants. Consecutive patients with CIDP and axonal PNPs were prospectively enrolled from the ward of the Department of Neurology at Huashan Hospital between March 2020 and March 2021. Inclusion criteria were diagnosis of CIDP or acquired axonal polyneuropathies (metabolic, toxic, or other known causes) according to the relevant diagnostic consensus criteria (3,17). The exclusion criteria were the following: (I) patients with additional neurologic diseases, such as Charcot-Marie-Tooth disease; (II) patients with severe lumbar disc herniation; (III) patients with MR imaging (MRI) contraindications or patients who were reluctant to undergo MRI examinations; and (IV) patients with an operation history or metal implantations in the lumbar region.

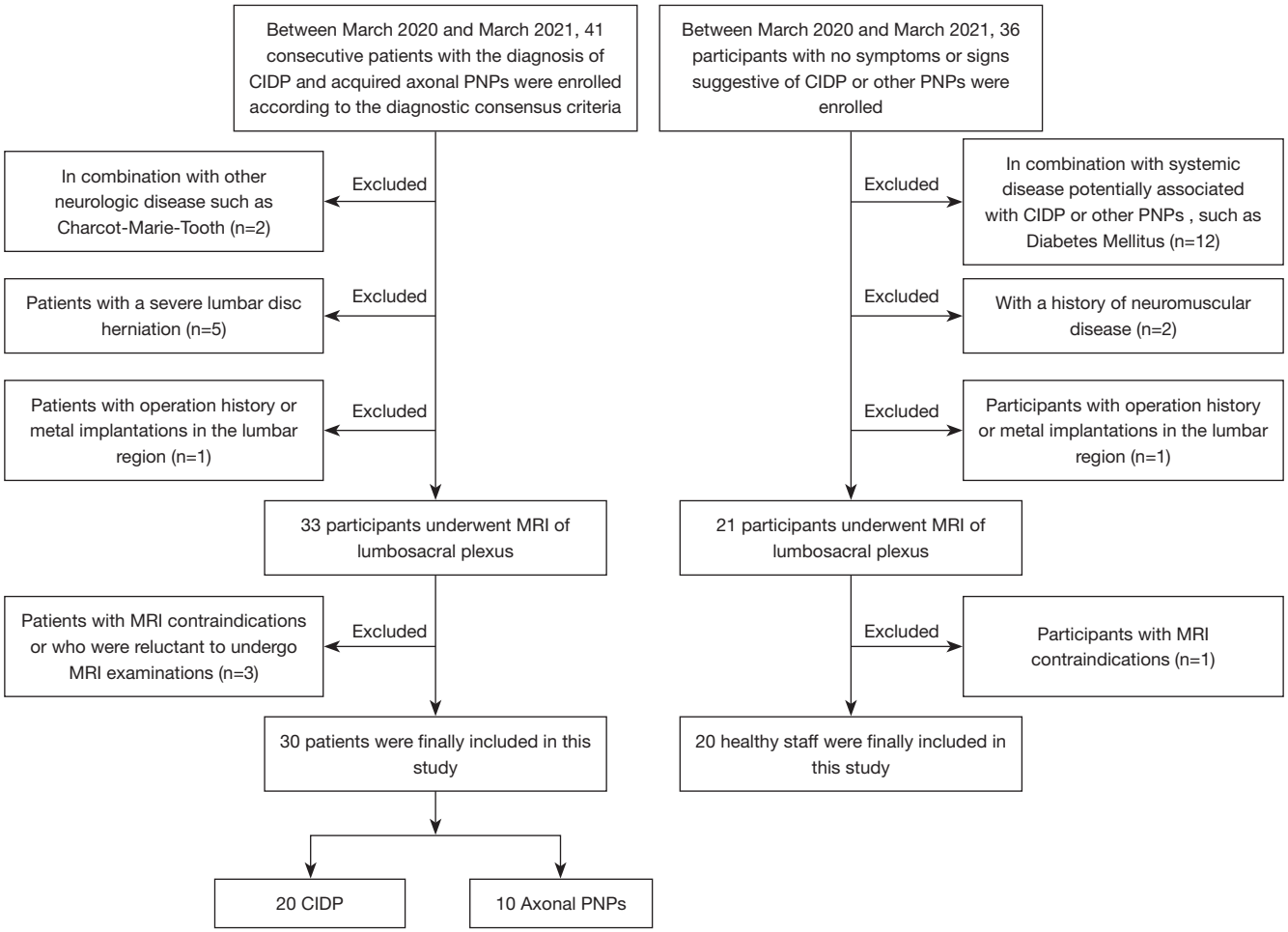

Figure 1 Flowchart of inclusions. CIDP, chronic inflammatory demyelinating polyneuropathy; PNP, polyneuropathy.

Healthy staff age matched to CIDP patients were recruited from the Huashan Hospital as the healthy control group. None had symptoms or signs suggestive of CIDP or other PNPs as assessed by physical examination. Participants with systemic disease potentially associated with CIDP or other PNPs (such as diabetes mellitus) or a history of neuromuscular disease were excluded. Participants with an operation history or metal implantations in the lumbar region or MRI contraindications were also excluded. A flowchart of inclusions is shown in *Figure 1*.

Information on baseline characteristics, including sex, age, disease duration, and cerebral spinal protein content were collected (*Table 1*), along with electrophysiological data.

MRN scanning

All participants were examined with a GE Discovery 3.0T scanner (GE Healthcare) using the following sequences: (I) sagittal T1WI fast spin echo (FSE) images for locating the nerve roots [repetition time (TR)/echo time (TE) =820/8.5 ms, field of view (FOV) =320×192 mm^2, matrix =352×256, thickness/gap =4/0.5 mm, 11 slices]; (II) coronal 3D T2WI FSE short-tau inversion recovery (STIR) for imaging of the lumbosacral plexus [TR/TE/inversion recovery (IR) =2,800/85/260 ms, thickness =2 mm, FOV =340×340 mm^2, matrix =384×288, 60 slices]; (III) axial single-shot spin echo planar imaging (EPI) DTI (TR/TE =5,212/85 ms, FOV =180×70 mm^2, matrix =128×90, thickness =3 mm, b value: 0 and 800 s/mm^2, 15 directions, 40 slices); and (IV) axial T2-weighted images of lumbosacral plexus acquired as an anatomic reference (TR/TE =8,185/120 ms, FOV =180×180 mm^2, matrix =256×192, thickness =3 mm, 40 slices).

The total acquisition time was 32 min and 18 s per

Table 1 Characteristics of all participants

Characteristics	CIDP (n=20)	Axonal PNPs (n=10)	Healthy controls (n=20)	P
Age (year)[a]	37.3±19.11	42.9±7.19	39.4±13.55	0.750
Male/female	16/4	8/2	11/9	0.211
Disease duration (month)[b]	14.50 (6.50, 35.25)	11.50 (5.00, 47.25)	–	0.775
CSF protein content (mg/L)[b]	760 (500, 2370)	637 (412, 1191.50)	–	0.313

[a], data are presented as mean ± standard deviation; [b], data are presented as median (interquartile range). CIDP, chronic inflammatory demyelinating polyneuropathy; PNP, polyneuropathy; CSF, cerebral spinal fluid.

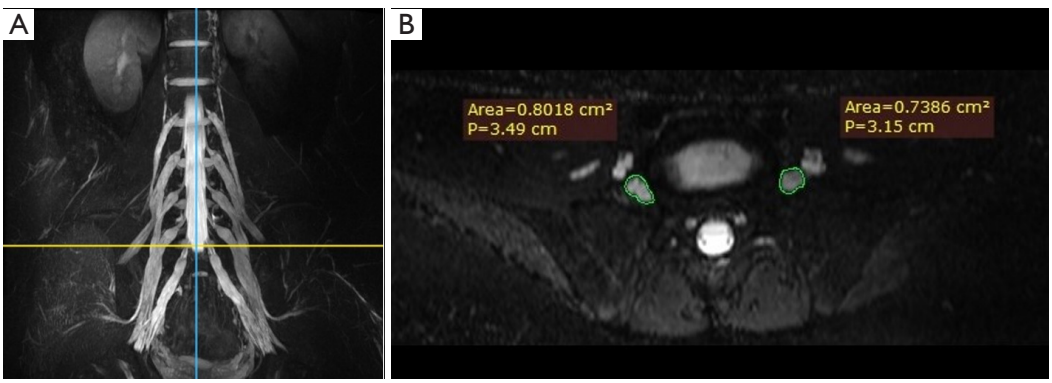

Figure 2 CSA measurement of the bilateral L5 nerve roots. (A) Maximum intensity projection of lumbosacral nerve roots in a patient with CIDP. The transverse line signifies the level of the L5/S1 intervertebral disc. (B) The reconstructed axial images on the corresponding level and ROIs placed manually around the boundary of the bilateral L5 nerve roots. CSA, cross-sectional area; CIDP, chronic inflammatory demyelinating polyneuropathy; ROI, region of interest.

subject.

Image postprocessing and measurement

The cross-sectional area (CSA) and diffusion parameters, including fractional anisotropy (FA) and apparent diffusion coefficient (ADC), were independently measured on a GE workstation by 2 radiologists with 3 and 5 years' experience in neuroradiology, respectively. Both radiologists were blinded to the clinical profile of all participants.

The CSA measurement of the bilateral L3 to S1 nerve roots was carried out on reconstructed axial 3D T2WI FSE STIR images. The procedure (taking the L5 nerve root as an example) was as follows: Regions of interest (ROIs) were placed manually around the boundary of the bilateral L5 nerve roots on level with the middle of the L5/S1 intervertebral disc, and the values were recorded. The same method was used to measure the CSAs of the bilateral L3, L4, and S1 nerve roots. Because of the obliquity of nerve roots, we used the average value of the 4 nerve roots as the CSA of the lumbosacral nerve roots, and this value was then employed for statistical analyses (*Figure 2*).

Measurement of FA and ADC values was carried out using FuncTool DTI processing software (ADW4.6, GE Healthcare). With axial T2WI images as an anatomic reference, each nerve root was divided into 3 levels: intraspinal, intraforaminal, and extraforaminal (18). Free-hand ROIs were placed to cover the entire visible signal on B0 images that were clearly differentiable as a nerve root at 3 levels, and FA and ADC values were recorded. The average measurements of the L4 to S1 nerve roots at 3 levels were recorded independently by the radiologists, and the mean value was used for statistical analyses (*Figure 3*).

Statistical analyses

Statistical analyses were performed on IBM SPSS (version 22.0, IMB Corp.). The Mann-Whitney *U* test was used to compare differences in disease duration and cerebral spinal fluid protein content in patients with CIDP and

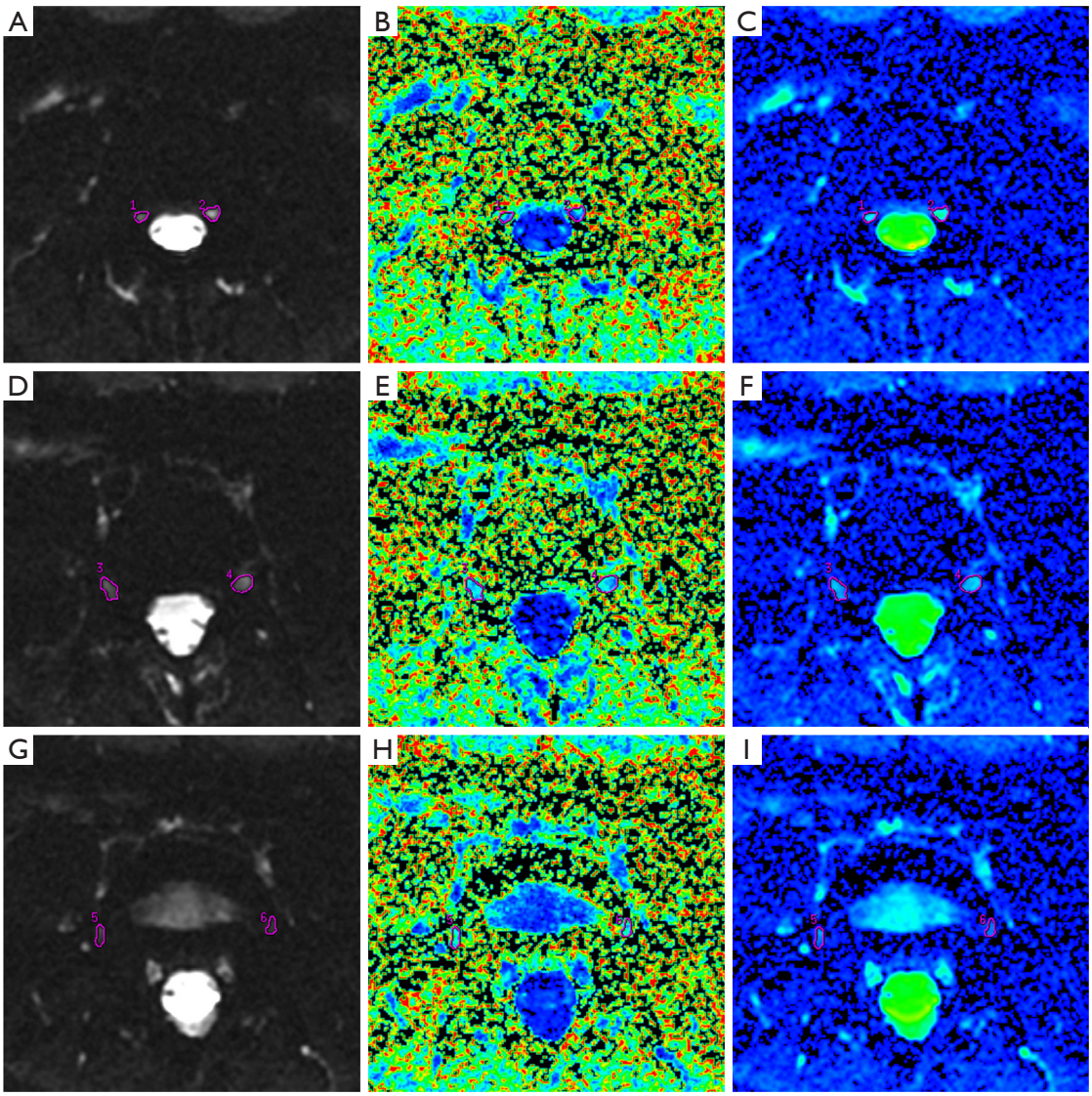

Figure 3 FA and ADC measurements of the bilateral L5 nerve roots. (A,D,G) B0 images on the level of the intraspinal region, intraforaminal region, and extraforaminal region. (B,E,H) FA maps on the level of the intraspinal region, intraforaminal region, and extraforaminal region. (C,F,I) ADC maps on the level of the intraspinal region, intraforaminal region, and extraforaminal region. FA, fractional anisotropy; ADC, apparent diffusion coefficient.

axonal PNPs. Kruskal-Wallis 1-way analysis of variance (ANOVA) was used to detect differences in CSA and diffusion parameters across the 3 groups (CIDP, axonal PNPs, and controls). A pairwise comparison was performed for further detailed analysis, and a P value of <0.05 after Bonferroni adjustment was considered significant. For the correlation analyses between disease duration and imaging parameters including CSA, FA and ADC, Pearson or Spearman correlation coefficients were used according to the normality of data. To evaluate the value of CSA and diffusion parameters in identifying CIDP and differentiating CIDP from axonal PNPs, receiver operating characteristic (ROC) curves were plotted and area under the curve (AUC) values were reported. The optimal cutoff values were also calculated using the Youden index, which was defined as follows: sensitivity + specificity − 1 (19). Combined ROC analysis was conducted with a combination of CSA and DTI parameters using a binary logistic equation. Interobserver

Table 2 CSA and diffusion parameters among the 3 groups

	CIDP	Axonal PNPs	Healthy controls	P	Pairwise comparisons (significance after Bonferroni adjustment)		
					P1	P2	P3
CSA (mm^2)	45.35±23.889	22.25±3.878	22.81±4.079	<0.001	<0.001	0.002	1.000
FA	0.24±0.053	0.27±0.014	0.32±0.045	<0.001	<0.001	0.578	0.022
ADC ($\times10^{-3}$ mm^2/s)	1.64±0.269	1.37±0.204	1.39±0.156	<0.001	0.005	0.015	1.000

P1: CIDP *vs.* healthy controls; P2: CIDP *vs.* axonal PNPs; P3: Axonal PNPs *vs.* healthy controls. Data are presented as mean ± standard deviation. CIDP, chronic inflammatory demyelinating polyneuropathy; PNP, polyneuropathy; CSA, cross-sectional area; FA, fractional anisotropy; ADC, apparent diffusion coefficient.

agreement regarding CSA and DTI parameters was calculated using intraclass correlation coefficient (ICC) and interpreted as follows: 0.8–1.0, excellent; 0.6–0.8, good; and <0.6, poor.

Results

Clinical data

A total of 20 patients with CIDP, 10 patients with axonal PNPs, and 20 healthy volunteers were enrolled in the study. The baseline characteristics are summarized in *Table 1*. In the CIDP group, 16 out of 20 patients were classified as typical CIDP, with symmetrical weakness and sensory deficit of 4 extremities for over 2 months, while the remaining 4 patients were classified as CIDP variant with atypical clinical presentations. Among the 4 CIDP variants, 3 patients were characterized by distal symmetrical sensorimotor symptoms and diagnosed with distal acquired demyelinating symmetric neuropathy. One patient presented with numbness of the lower extremities for 4 months without motor symptoms and was diagnosed with pure sensory CIDP. At the time of the study, 14 patients had received treatments, including intravenous immunoglobulin, steroids, and plasma exchange. In patients with axonal PNPs, the etiologies included diabetes mellitus (n=5), chemotherapy (n=2), primary Sjögren's syndrome (n=2), and chronic alcoholism (n=1). Correlation analyses showed there were no significant correlations between disease duration and CSA (P=0.883), FA (P=0.452), or ADC (P=0.833).

The electrophysiological data of patients with CIDP and axonal PNPs are presented in Table S1. All CIDP patients showed demyelination in at least 1 motor nerve of the lower extremities. In addition, 8 of 20 patients showed secondary axonal damage according to nerve conduction study data. All 10 patients with axonal PNPs showed axonal injury in at least 1 lower extremity nerve.

Interobserver agreement of CSA and DTI parameters

The ICC values for CSA, FA, and ADC were 0.986 [95% confidence interval (95% CI): 0.976–0.992], 0.894 (95% CI: 0.747–0.912), and 0.837 (95% CI: 0.727–0.904), respectively, indicating excellent interobserver agreement.

CSA and DTI parameters of lumbosacral nerve roots among the 3 groups

The CSA values for CIDP, axonal PNPs, and healthy controls were 45.35±23.889, 22.25±3.878, and 22.81±4.079 mm^2, respectively. Patients with CIDP exhibited significantly increased CSA values of lumbosacral nerve roots compared to those with axonal PNPs (P=0.002) and healthy controls (P<0.001). The FA values for CIDP, axonal PNPs, and healthy controls were 0.24±0.053, 0.27±0.014, and 0.32±0.045, respectively; the ADC values were $(1.64\pm0.269)\times10^{-3}$, $(1.37\pm0.204)\times10^{-3}$, and $(1.39\pm0.156)\times10^{-3}$ mm^2/s, respectively. Compared with healthy controls, CIDP patients demonstrated significantly decreased FA and increased ADC values (P<0.001 and P=0.005, respectively), while axonal PNPs only showed lower FA value (P=0.022). Compared with axonal PNPs, CIDP patients showed significantly increased ADC (P=0.015), with unchanged FA (P=0.578). The details are shown in *Table 2* and *Figure 4*.

ROC analysis of CSA and DTI parameters in the diagnosis and differential diagnosis of CIDP

In differentiating CIDP from healthy controls, the AUC values of CSA, FA, and ADC were 0.858 (95% CI: 0.711–0.948), 0.904 (95% CI: 0.768–0.974), and 0.791 (95% CI: 0.634–0.903), respectively (all P values <0.001). When the CSA value of lumbosacral nerve roots reached 28.15 mm^2, it

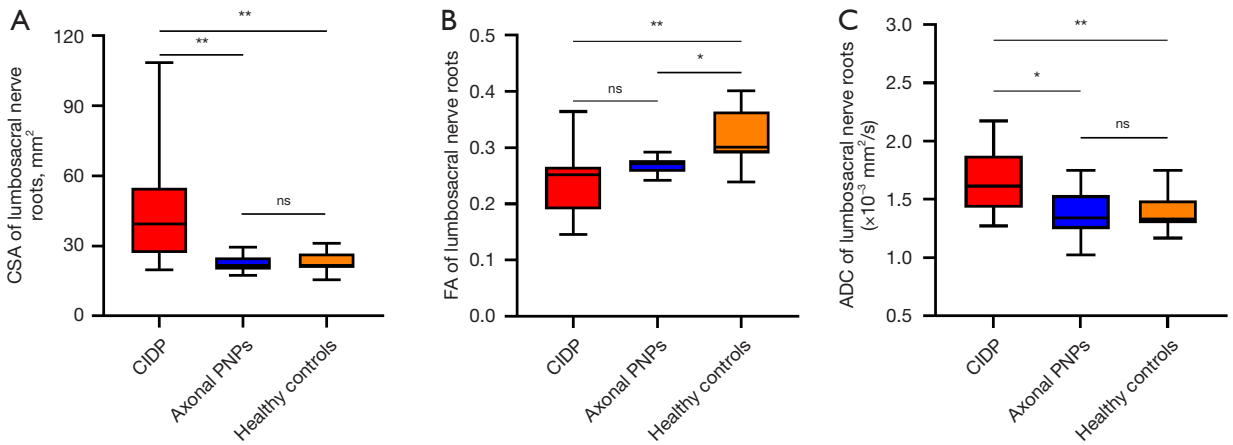

Figure 4 CSA and DTI parameters in the CIDP, axonal PNP, and healthy control groups. *P<0.05, **P<0.01; ns, not significant; CSA, cross-sectional area; DTI, diffusion tensor imaging; FA, fractional anisotropy; ADC, apparent diffusion coefficient; CIDP, chronic inflammatory demyelinating polyneuropathy; PNP, polyneuropathy.

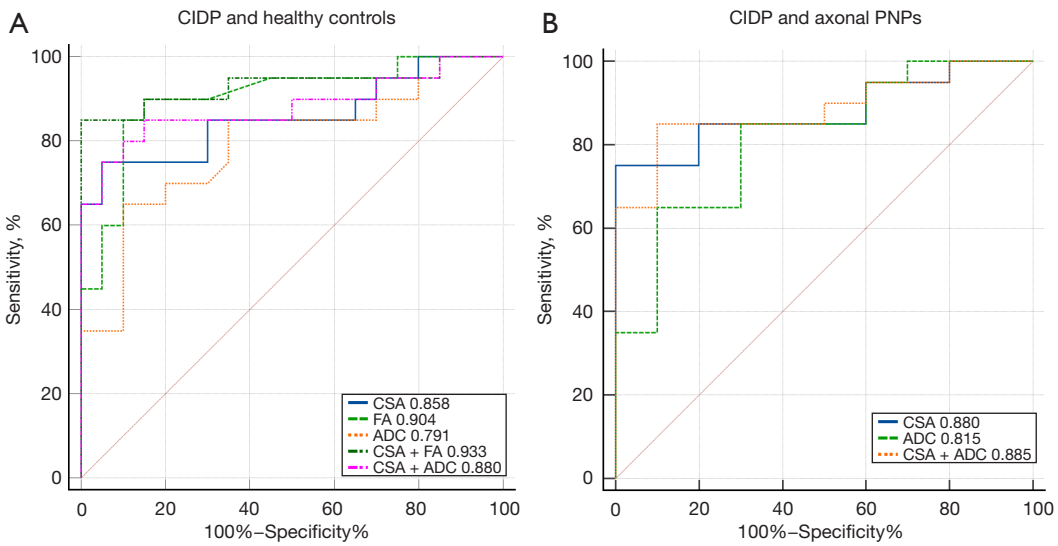

Figure 5 ROC curves of MRN in identifying CIDP (A) and differentiating it from axonal PNPs (B). ROC, receiver operating characteristic; MRN, magnetic resonance neurography; CIDP, chronic inflammatory demyelinating polyneuropathy; PNP, polyneuropathy.

could provide a sensitivity and specificity of 75% and 95%, respectively. Compared with ADC, FA had a larger AUC value, and its optimal cutoff value was 0.278, with a sensitivity and specificity of 85% and 90%, respectively. A combination of CSA and FA had an AUC of 0.933 (95% CI: 0.806–0.987), and a combination of CSA and ADC had an AUC of 0.880 (95% CI: 0.738–0.961; *Figure 5* and Table S2).

In differentiating CIDP from axonal PNPs, the AUC values of CSA and ADC were 0.880 (95% CI: 0.709–0.969) and 0.815 (95% CI: 0.631–0.932), respectively (both P value <0.001). When the CSA value of lumbosacral nerve roots reached 29.46 mm^2, it could provide a sensitivity and specificity of 75% and 100%, respectively. When the ADC value was 1.576×10^{-3} mm^2/s, the sensitivity and specificity were 65% and 90%, respectively. A combination of CSA and ADC had an AUC of 0.885 (95% CI: 0.716–0.972; *Figure 5* and Table S2).

Additionally, the FA value could be used to differentiate axonal PNPs from healthy controls with a cutoff value of 0.279 and a sensitivity and specificity of 90%.

Discussion

This MRN study demonstrated significant differences in CSA and diffusion parameters of lumbosacral nerve roots in patients with CIDP and axonal PNPs as well as in healthy controls, which could be used to identify patients with CIDP and further distinguish them from patients with axonal PNPs.

In previous HRUS studies, assessment of the nerve size of 4 extremities in PNPs found pronounced generalized nerve enlargement in demyelinating PNPs, while no or slight enlargement was seen in axonal PNPs (5,20,21). Scheidl *et al.* measured CSA values of the C5–C7 nerve roots and several upper and lower limb nerves in patients with acquired demyelinating and axonal PNPs as well as in healthy controls, reporting that the 2 types of PNPs were characterized by different patterns of nerve enlargement (7). Research indicates that demyelinating PNPs, especially CIDP, exhibit nerve enlargement in a proximally predominating pattern, whereas in axonal PNPs, nerve enlargement is prone to occur in distal segments, if any. This differential distribution of nerve enlargement actually reflects the length-dependent nature of axonal PNPs and the preferential and predominant involvement of proximal nerve roots and segments in acquired demyelinating PNPs, in particular CIDP (7,22-24). Based on this observation, this study used MRI to visualize the lumbosacral nerve roots where ultrasound was not accessible, and quantified the mean size among 3 groups. As expected, a significantly increased CSA of the lumbosacral nerve roots was only found in patients with CIDP, whereas no difference was observed between patients with axonal PNPs and healthy controls. Evaluation of diagnostic performance showed that the application of the CSA of lumbosacral nerve roots in identifying CIDP and differentiating it from axonal PNPs was satisfactory, with ROC analysis providing a relatively high AUC (0.858 and 0.880, respectively). The optimal cutoff values together with the sensitivity and specificity were also obtained and could serve as a clinical reference. These results complement previous HRUS studies which did not measure the size of the lumbosacral nerve roots and can provide additional valuable information in diagnosing CIDP, especially in cases where electrophysiological results are equivocal or substantial secondary axonal degeneration has occurred.

Another important finding was the difference in diffusion parameters of the lumbosacral nerve roots across the 3 groups, which had not been explored in detail prior to this study. As another imaging modality of MRN, DTI can provide information about the microstructure characteristics of nerve fibers by yielding diffusion parameters (25). FA, the most commonly used metric, measures the degree of anisotropic diffusion and reflects the arrangement and integrity of the cellular structure within nerve fibers. A decrease in FA often indicates the disruption of well-organized cellular architecture (26). ADC represents the extent of water diffusion and is increased in individuals with inflammation, trauma, or tumors (27). In this study, patients with CIDP exhibited a significantly lower FA value and higher ADC value than did healthy volunteers, which was consistent with the results of previous studies (13,28). This finding could be explained by the pathologic processes of demyelination, inflammatory cell infiltration, and endoneurial edema in CIDP (24,29). Furthermore, we found that the FA value of lumbosacral nerve roots was lower in patients with axonal PNPs than in healthy controls but that the ADC did not differ significantly between the 2 groups. Axonal PNPs, as mentioned above, are characterized by axonal injury mainly in distal nerve segments. Correspondingly, previous studies have demonstrated a decreased FA value and increased ADC value in lower extremity nerves (30-32). The proximal lumbosacral nerve roots, however, have never been covered. Pathologically, the axonal injury can progress from the distal segment to the proximal segment in a "dying-back" pattern (23). In this study, the disease duration of patients with axonal PNPs was relatively long (the median disease duration was 11.50 months), and consequently, the proximal nerve roots were likely to be involved, which might account for the decrease in FA value. Of note, in this study, axonal PNPs did not exhibit morphological alterations but showed decreased FA value of the lumbosacral nerve roots when compared to healthy controls, which suggests that the FA was sufficiently sensitive to detect the microstructure change of nerve fibers even if no abnormality was seen in conventional MRI. As for ADC value, it remained unchanged in patients with axonal PNPs compared with healthy controls, possibly because it was less sensitive than FA. Pairwise comparison showed no statistical difference in the FA value between patients with CIDP and those with axonal PNPs, which suggests the FA value decreased in both the CIDP and axonal PNPs and thus could not be used to distinguish the 2 types of PNPs. ADC, on the contrary, showed satisfactory efficacy in identifying CIDP (AUC =0.791) and distinguishing it from axonal PNPs and (AUC =0.815). The combined ROC analysis showed that a combination of CSA and ADC could further improve the diagnostic performance.

Our study had several limitations. First, the number of patients with axonal PNPs was relatively small. Second, the patient cohort in this study came from a single center. However, this was an exploratory study and our results showed the feasibility of MRN in identifying CIDP and distinguishing it from axonal PNPs. In the future, we will further expand the patient cohort to verify the current results.

In conclusion, the CSA and ADC values of lumbosacral nerve roots helped to identify patients with CIDP and further distinguish them from patients with axonal PNPs. FA value decreased in both types of PNP and had limited value in the discriminating between these 2 types.

Acknowledgments

Funding: This work was supported by the Shanghai Science and Technology Commission (No. 18411967300) and the Natural Science Foundation of Shanghai (No. 20ZR1409300).

Footnote

Reporting Checklist: The authors have completed the STROBE reporting checklist. Available at https://qims.amegroups.com/article/view/10.21037/qims-22-156/rc

Conflicts of Interest: All authors have completed the ICMJE uniform disclosure form (available at https://qims.amegroups.com/article/view/10.21037/qims-22-156/coif). The authors have no conflicts of interest to declare.

Ethical Statement: The authors are accountable for all aspects of the work in ensuring that questions related to the accuracy or integrity of any part of the work are appropriately investigated and resolved. This study was conducted in accordance with the Declaration of Helsinki (as revised in 2013). The study was approved by the institutional ethics board of Huashan Hospital, and informed consent was provided by all the patients.

References

1. Bunschoten C, Jacobs BC, Van den Bergh PYK, Cornblath DR, van Doorn PA. Progress in diagnosis and treatment of chronic inflammatory demyelinating polyradiculoneuropathy. Lancet Neurol 2019;18:784-94.
2. Latov N. Diagnosis and treatment of chronic acquired demyelinating polyneuropathies. Nat Rev Neurol 2014;10:435-46.
3. Van den Bergh PY, Hadden RD, Bouche P, Cornblath DR, Hahn A, Illa I, Koski CL, Léger JM, Nobile-Orazio E, Pollard J, Sommer C, van Doorn PA, van Schaik IN; Peripheral Nerve Society. European Federation of Neurological Societies/Peripheral Nerve Society guideline on management of chronic inflammatory demyelinating polyradiculoneuropathy: report of a joint task force of the European Federation of Neurological Societies and the Peripheral Nerve Society - first revision. Eur J Neurol 2010;17:356-63.
4. Vallat JM, Sommer C, Magy L. Chronic inflammatory demyelinating polyradiculoneuropathy: diagnostic and therapeutic challenges for a treatable condition. Lancet Neurol 2010;9:402-12.
5. Grimm A, Heiling B, Schumacher U, Witte OW, Axer H. Ultrasound differentiation of axonal and demyelinating neuropathies. Muscle Nerve 2014;50:976-83.
6. Pham M, Bäumer T, Bendszus M. Peripheral nerves and plexus: imaging by MR-neurography and high-resolution ultrasound. Curr Opin Neurol 2014;27:370-9.
7. Scheidl E, Böhm J, Simó M, Bereznai B, Bereczki D, Arányi Z. Different patterns of nerve enlargement in polyneuropathy subtypes as detected by ultrasonography. Ultrasound Med Biol 2014;40:1138-45.
8. Rajabally YA, Morlese J, Kathuria D, Khan A. Median nerve ultrasonography in distinguishing neuropathy subtypes: a pilot study. Acta Neurol Scand 2012;125:254-9.
9. Oudeman J, Eftimov F, Strijkers GJ, Schneiders JJ, Roosendaal SD, Engbersen MP, Froeling M, Goedee HS, van Doorn PA, Caan MWA, van Schaik IN, Maas M, Nederveen AJ, de Visser M, Verhamme C. Diagnostic accuracy of MRI and ultrasound in chronic immune-mediated neuropathies. Neurology 2020;94:e62-74.
10. Chhabra A, Madhuranthakam AJ, Andreisek G. Magnetic resonance neurography: current perspectives and literature review. Eur Radiol 2018;28:698-707.
11. Sneag DB, Queler S. Technological Advancements in Magnetic Resonance Neurography. Curr Neurol Neurosci

Rep 2019;19:75.
12. Wu F, Wang W, Zhao Y, Liu B, Wang Y, Yang Y, Ren Y, Liu H. MR neurography of lumbosacral nerve roots: Diagnostic value in chronic inflammatory demyelinating polyradiculoneuropathy and correlation with electrophysiological parameters. Eur J Radiol 2020;124:108816.
13. Kronlage M, Pitarokoili K, Schwarz D, Godel T, Heiland S, Yoon MS, Bendszus M, Bäumer P. Diffusion Tensor Imaging in Chronic Inflammatory Demyelinating Polyneuropathy: Diagnostic Accuracy and Correlation With Electrophysiology. Invest Radiol 2017;52:701-7.
14. Kronlage M, Bäumer P, Pitarokoili K, Schwarz D, Schwehr V, Godel T, Heiland S, Gold R, Bendszus M, Yoon MS. Large coverage MR neurography in CIDP: diagnostic accuracy and electrophysiological correlation. J Neurol 2017;264:1434-43.
15. Lichtenstein T, Sprenger A, Weiss K, Slebocki K, Cervantes B, Karampinos D, Maintz D, Fink GR, Henning TD, Lehmann HC. MRI biomarkers of proximal nerve injury in CIDP. Ann Clin Transl Neurol 2017;5:19-28.
16. Eftimov F, Lucke IM, Querol LA, Rajabally YA, Verhamme C. Diagnostic challenges in chronic inflammatory demyelinating polyradiculoneuropathy. Brain 2020;143:3214-24.
17. Preston D, Shapiro B. Electromyography and neuromuscular disorders, clinical-electrophysiological correlations. New York: Elsevier Saunders; 2013.
18. Wang X, Wang H, Sun C, Zhou S, Meng T, Lv F, Ma X, Xia X, Jiang J. Analysis of radiological parameters associated with decreased fractional anisotropy values on diffusion tensor imaging in patients with lumbar spinal stenosis. Eur Spine J 2019;28:1397-405.
19. Youden WJ. Index for rating diagnostic tests. Cancer 1950;3:32-5.
20. Zaidman CM, Al-Lozi M, Pestronk A. Peripheral nerve size in normals and patients with polyneuropathy: an ultrasound study. Muscle Nerve 2009;40:960-6.
21. Goedee HS, van der Pol WL, van Asseldonk JH, Franssen H, Notermans NC, Vrancken AJ, van Es MA, Nikolakopoulos S, Visser LH, van den Berg LH. Diagnostic value of sonography in treatment-naive chronic inflammatory neuropathies. Neurology 2017;88:143-51.
22. Samuelsson K, Press R. Chronic axonal idiopathic polyneuropathy: is it really benign. Curr Opin Neurol 2020;33:562-7.
23. McCorquodale D, Smith AG. Clinical electrophysiology of axonal polyneuropathies. Handb Clin Neurol 2019;161:217-40.
24. Mathey EK, Park SB, Hughes RA, Pollard JD, Armati PJ, Barnett MH, Taylor BV, Dyck PJ, Kiernan MC, Lin CS. Chronic inflammatory demyelinating polyradiculoneuropathy: from pathology to phenotype. J Neurol Neurosurg Psychiatry 2015;86:973-85.
25. Jeon T, Fung MM, Koch KM, Tan ET, Sneag DB. Peripheral nerve diffusion tensor imaging: Overview, pitfalls, and future directions. J Magn Reson Imaging 2018;47:1171-89.
26. Budzik JF, Balbi V, Verclytte S, Pansini V, Le Thuc V, Cotten A. Diffusion tensor imaging in musculoskeletal disorders. Radiographics 2014;34:E56-72.
27. Jambawalikar S, Baum J, Button T, Li H, Geronimo V, Gould ES. Diffusion tensor imaging of peripheral nerves. Skeletal Radiol 2010;39:1073-9.
28. Markvardsen LH, Vaeggemose M, Ringgaard S, Andersen H. Diffusion tensor imaging can be used to detect lesions in peripheral nerves in patients with chronic inflammatory demyelinating polyneuropathy treated with subcutaneous immunoglobulin. Neuroradiology 2016;58:745-52.
29. Rizzuto N, Morbin M, Cavallaro T, Ferrari S, Fallahi M, Galiazzo Rizzuto S. Focal lesions area feature of chronic inflammatory demyelinating polyneuropathy (CIDP). Acta Neuropathol 1998;96:603-9.
30. Schneider C, Sprenger A, Weiss K, Slebocki K, Maintz D, Fink GR, Henning TD, Lehmann HC, Lichtenstein T. MRI detects peripheral nerve and adjacent muscle pathology in non-systemic vasculitic neuropathy (NSVN). J Neurol 2019;266:975-81.
31. Vaeggemose M, Haakma W, Pham M, Ringgaard S, Tankisi H, Ejskjaer N, Heiland S, Poulsen PL, Andersen H. Diffusion tensor imaging MR Neurography detects polyneuropathy in type 2 diabetes. J Diabetes Complications 2020;34:107439.
32. Wu C, Wang G, Zhao Y, Hao W, Zhao L, Zhang X, Cao J, Wang S, Chen W, Chan Q, Zhao B, Chhabra A. Assessment of tibial and common peroneal nerves in diabetic peripheral neuropathy by diffusion tensor imaging: a case control study. Eur Radiol 2017;27:3523-31.

Cite this article as: Wu F, Wang W, Yang Y, Li C, Wu J, Liu H, Ren Y. MR neurography of lumbosacral nerve roots for differentiating chronic inflammatory demyelinating polyneuropathy from acquired axonal polyneuropathies: a cross-sectional study. Quant Imaging Med Surg 2022;12(10):4875-4884. doi: 10.21037/qims-22-156

